(*R*)-3-Hydroxybutyrate Dehydrogenase: Selective Phosphatidylcholine Binding by the C-Terminal Domain†

Christine Loeb-Hennard and J. Oliver McIntyre*

Department of Biological Sciences, Vanderbilt University, Nashville, Tennessee 37235

Received February 23, 2000; Revised Manuscript Received June 2, 2000

ABSTRACT: (*R*)-3-Hydroxybutyrate dehydrogenase (BDH) is a lipid-requiring mitochondrial enzyme that has a specific requirement of phosphatidylcholine (PC) for function. The C-terminal domain (CTBDH) of human heart BDH (residues 195−297) has now been expressed in *Escherichia coli* as a chimera with a soluble protein, glutathione *S*-transferase (GST), yielding GST-CTBDH, a novel fusion protein that has been purified and shown to selectively bind to PC vesicles. Both recombinant human heart BDH (HH-Histag-BDH) and GST-CTBDH (but not GST) form well-defined protein−lipid complexes with either PC or phosphatidylethanolamine (PE)/diphosphatidylglycerol (DPG) vesicles (but not with digalactosyl diglyceride vesicles) as demonstrated by flotation in sucrose gradients. The protein−PC complexes are stable to 0.5 M NaCl, but complexes of either HH-Histag-BDH or GST-CTBDH with PE/DPG vesicles are dissociated by salt treatment. Thrombin cleavage of GST-CTBDH, either before or after reconstitution with PC vesicles, yields CTBDH (12 111 Da by MALDI mass spectrometry) which retains lipid binding without attached GST. The BDH activator, 1-palmitoyl-2-(1-pyrenyl)decanoyl-PC (pyrenyl-PC), at <2.5% of total phospholipid in vesicles, efficiently quenches a fraction (0.36 and 0.47, respectively) of the tryptophan fluorescence of both HH-Histag-BDH and GST-CTBDH with effective Stern−Volmer quenching constants, $(K_Q)_{eff}$, of 11 and 9.3 $(\%)^{-1}$, respectively (half-maximal quenching at ∼0.1% pyrenyl-PC). Maximal quenching by pyrenyl-PC obtains at approximately stoichiometric pyrenyl-PC to protein ratios, reflecting high-affinity interaction of pyrenyl-PC with both HH-Histag-BDH and GST-CTBDH. The analogous pyrenyl-PE effects a similar maximal quenching of tryptophan fluorescence for both proteins but with ∼15-fold lower $(K_Q)_{eff}$ (half-maximal quenching at ∼1.5% pyrenyl-PE) referable to nonspecific interaction of pyrenyl-PE with HH-Histag-BDH or GST-CTBDH. Thus, the 103-residue CTBDH constitutes a PC-selective lipid binding domain of the PC-requiring BDH.

(*R*)-3-Hydroxybutyrate dehydrogenase (BDH;[1] EC 1.1.1.30) is a mitochondrial enzyme located on the matrix face of the inner membrane (*1*). With NAD(H) as coenzyme, BDH catalyzes the interconversion of acetoacetate and (*R*)-3-hydroxybutyrate, the two major "ketone bodies" produced during fatty acid catabolism. BDH has a specific requirement of phosphatidylcholine (PC) for activity (*2*−*5*) and exhibits cooperative PC-dependent activation (*6*). An allosteric mechanism has been identified whereby PC enhances NAD(H) binding to BDH (*7*). The hydrophobic moiety of PC is important for the activation of BDH (*3*, *4*, *8*), though the enzyme exhibits little structural specificity for that part of the PC molecule (*9*). By contrast, there is a high degree of specificity for the phosphocholine moiety that can be varied only within limits of steric and structural constraints (*9*). Other lipids that contain this moiety, e.g., sphingomyelin and lysolecithin, can also partially activate BDH (10−30%), but complexes with such lipids are unstable as compared with PC complexes (*9*). Indeed, in early studies it was recognized that the stability of the BDH−lipid activator complex depends strongly on the aggregation state of the lipid; e.g., lipids that form stable fluid bilayers are preferred (*4*) whereas micellar lipids inactivate the enzyme (*4*, *8*). BDH also readily forms complexes with lipids other than PC, such as phos-

† These studies were supported by the National Institutes of Health, Grant DK49186, and by pilot funds from the Clinical Nutrition Research Unit of Vanderbilt Medical Center, Grant DK26657.

* To whom correspondence should be addressed. Tel: 615-343-3368. Fax: 615-343-6833. E-mail: oliver.mcintyre@vanderbilt.edu.

[1] Abbreviations: BDH, (*R*)-3-hydroxybutyrate dehydrogenase; buffer B, 20 mM Hepes−NaOH (pH 8.0) and 1 mM EDTA; CHAPS, 3-[(3-cholamidopropyl)dimethylammonio]-1-propanesulfonate; CTBDH, C-terminal domain of BDH (residues 195−297); DGDG, digalactosyl diglyceride; DPG, diphosphatidylglycerol; DTT, dithiothreitol; EDTA, ethylenediaminetetraacetic acid; $(f_a)_{eff}$, fraction of fluorescence accessible to quencher; GST, glutathione *S*-transferase; GST-CTBDH, fusion protein of glutathione *S*-transferase with the C-terminal domain of BDH (residues 195−297); Hepes, 4-(2-hydroxyethyl)-1-piperazineethanesulfonic acid; HDN buffer, 5 mM Hepes−NaOH (pH 8.0), 2 mM DTT, and 0.1 M NaCl; HH, human heart; HH-Histag-BDH, fusion protein of HH-BDH with a 17-residue N-terminal fusion peptide containing a hexahistidine sequence; HPLC, high-performance liquid chromatography; IPTG, isopropyl β-D-1-thiogalactopyranoside; $(K_Q)_{eff}$, effective Stern−Volmer fluorescence quenching constant; MALDI, matrix-assisted laser desorption ionization; MPL, mitochondrial phospholipids; NAD(H), nicotinamide adenine dinucleotide (reduced); PAGE, polyacrylamide gel electrophoresis; PBS buffer, 140 mM NaCl, 2.7 mM KCl, 10 mM Na_2HPO_4, and 1.8 mM KH_2PO_4 (pH 7.3); PC, phosphatidylcholine; PCR, polymerase chain reaction; PE, phosphatidylethanolamine; PMSF, phenylmethanesulfonyl fluoride; pyrenyl-PC, 1-palmitoyl-2-(1-pyrenyl)decanoyl-*sn*-glycero-3-phosphocholine; pyrenyl-PE, 1-palmitoyl-2-(1-pyrenyl)decanoyl-*sn*-glycero-3-phosphoethanolamine; SCADH, short-chain alcohol dehydrogenase; STE buffer, 10 mM Tris-HCl (pH 8.0), 150 mM NaCl, and 1 mM EDTA; TFA, trifluoroacetic acid; Tris, 2-amino-2-(hydroxymethyl)-1,3-propanediol.

10.1021/bi000425y CCC: $19.00 © 2000 American Chemical Society
Published on Web 09/07/2000

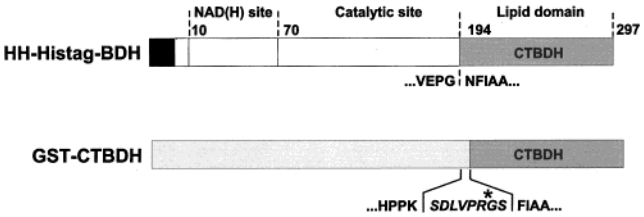

FIGURE 1: Domain structures of HH-Histag-BDH and GST-CTBDH. HH-Histag-BDH (upper) consists of the three domains of HH-BDH, the NAD(H) site, the catalytic site, and the lipid binding domain (CTBDH), with a polyhistidine tag (depicted by the black box) linked at the N-terminus [see Chelius et al. (*14*)]. The lengths of each bar are approximately proportional to the number of amino acids in each segment, with the beginning residue of each domain denoted by the numbers above the bar (based on the sequence for mature HH-BDH; see ref 12) and residues 194−297 being CTBDH. The amino acid sequence at the catalytic to lipid domain boundary is shown below. GST-CTBDH (lower) consists of GST, a linker, and CTBDH. The segment of amino acid sequence shown below GST-CTBDH includes the last four residues of GST and the linker (eight residues shown in italics), followed by the first four residues of CTBDH (beginning at residue 195 of HH-BDH). The linker contains the thrombin recognition site (LVPRGS) that provides thrombin-specific cleavage (denoted by the asterisk) of GST-CTBDH following the R residue.

phatidylethanolamine (PE) and/or diphosphatidylglycerol (DPG), two other major mitochondrial lipids, but these do not reactivate enzymic function (*3*). Thus, the binding of phospholipid to BDH is a necessary but not sufficient requisite for enzymic activity (*3*), and lipid binding, per se, does not reflect the lipid specificity for BDH activation. The specificity of BDH for PC is, however, manifest in the relative stability of the active BDH−PC complex which is not dissociated by the addition of salt. By contrast, such treatment dissociates complexes with nonactivating lipids such as PE/DPG in which the BDH−lipid interaction appears to be predominantly ionic and nonspecific (*3*). In the studies described here, the differential salt stability of protein−PC versus protein−PE/DPG complexes has been utilized to characterize the PC-selective lipid vesicle binding properties of both recombinant HH-BDH and its C-terminal domain.

The mature form of BDH consists of 297 amino acid residues for both the human heart (*10*) and rat liver enzymes (*11*) which have ~90% identity (*12*). Sequence homology with other short-chain alcohol dehydrogenases (SC-ADH) (*13*) predicts that the N-terminal two-thirds of BDH includes both putative NAD(H) binding and catalytic sites (*10*). These two active site domains of BDH have been confirmed recently by structure prediction modeling (*14*) based on the 3D structures of two related SC-ADH (*15*, *16*). The C-terminal domain of BDH (identified originally as residues 194−297; see Figure 1) shows limited sequence homology with SC-ADH or any other protein and has been predicted to confer substrate specificity and phospholipid binding (*10*). The postulated role for the C-terminal domain in the PC-dependent activation of BDH (*10*) has been supported by studies of C-terminally truncated forms of the enzyme that have altered interactions with lipid and/or minimal activity (*12*, *17*, *18*).

This paper characterizes the lipid binding properties of a recently described recombinant human heart BDH (HH-Histag-BDH) (*14*) and of a fusion protein consisting of the C-terminal domain of BDH, CTBDH (residues 195−297), fused at its N-terminus via a linker peptide to glutathione *S*-transferase (GST). This novel fusion protein, GST-CTBDH, was designed, expressed, purified, and characterized so as to test the hypothesis that the C-terminal segment of BDH is a novel PC-selective lipid binding domain of this PC-requiring enzyme. Both GST-CTBDH and HH-Histag-BDH are shown to form well-defined salt-stable complexes with PC vesicles but salt-dissociable complexes with PE/DPG vesicles. In addition, both HH-Histag-BDH and GST-CTBDH exhibit a similar high affinity for PC in lipid bilayers (as determined from the tryptophan fluorescence quenching afforded by titration with pyrenyl-PC in lipid bilayers) and an order of magnitude lower affinity for the analogous pyrenyl-PE, a lipid that does not activate BDH. These studies demonstrate that CTBDH is sufficient to constitute the PC-selective lipid binding domain of BDH.

EXPERIMENTAL PROCEDURES

Materials. Buffer compounds and substrates were of analytical grade from various commercial sources. Diphosphatidylglycerol (DPG, bovine heart), synthetic 1,2-dioleoylphosphatidylcholine (PC), and 1,2-dioleoylphosphatidylethanolamine (PE) were from Avanti Polar Lipids (Alabaster, AL). Digalactosyl diglyceride (DGDG, whole wheat) was from Serdary Research Laboratories (Ontario, Canada). Pyrenyl-PC was purchased from Molecular Probes (Eugene, OR). NAD^+ was obtained from Schweizerhall (Piscataway, NJ). *n*-Octyl glucoside was from Calbiochem (La Jolla, CA). Restriction enzymes were from Promega (Madison, WI). Anti-GST goat antibodies were from Pharmacia Biotech (Piscataway, NJ). Alkaline phosphatase conjugated anti-rabbit antibodies were from Promega (Madison, WI) and AP anti-goat antibodies from Pierce (Rockford, IL). Lyophilized thrombin was from Pharmacia Biotech (Piscataway, NJ). Cytochrome *c* from horse heart (type VI, C7752) was from Sigma (St. Louis, MO). Protein molecular mass standards for SDS−PAGE were from Bio-Rad (Hercules, CA) (97−14 kDa low range) or from Life Technologies (Gibco BRL Products, Grand Island, NY) (43.0−2.3 kDa). Prestained SDS−PAGE protein standards were from Bio-Rad (104−19 kDa low range or 202−6.9 kDa kaleidoscope standards).

Analytical Methods. Protein was assayed by the method of Lowry et al. (*19*) as described (*7*). GST activity was measured following the protocol provided by Pharmacia Biotech (Piscataway, NJ), i.e., at room temperature (~23 °C) in 0.1 M potassium phosphate buffer (pH 6.5) with 1-chloro-2,4-dinitrobenzene and reduced glutathione as substrates, and activity units are expressed as the rate of product formation (micromoles per minute).

Preparation of HH-Histag-BDH. HH-Histag-BDH was expressed and purified using a modification (Loeb-Hennard, Goldthwaite, and McIntyre, unpublished) of the procedure described by Chelius et al. (*14*).

Construction of GST-CTBDH Expression Plasmid. To construct the expression plasmid for the GST-CTBDH fusion protein, the cDNA encoding CTBDH [from pBDHVU1; Chelius et al. (*14*)] was modified to create *Bam*HI and *Eco*RI sites at the 5′ and 3′ ends for subsequent ligation into the pGEX2T vector (Pharmacia Biotech, Piscataway, NJ). Unless noted otherwise, DNA methodology was as described by Sambrook et al. (*20*). For PCR reaction, primers had the

following sequences: CCC**GGATCC**TTCATCGCTGCCACCAGC (primer 1) and TT**GAATTC**AGCGGATGTAGATCATGTCGGA (primer 2). *Bam*HI and *Eco*RI sites in primers 1 and 2, respectively, are shown in bold, and the *Eco*RI site in primer 2 (complementary strand) immediately follows the stop codon present in HH-BDH cDNA. The PCR reaction was performed using the Expand High Fidelity system (Boehringer-Mannheim, Indianapolis, IN) in a DNA thermal cycler (Perkin-Elmer-Cetus, Perkin-Elmer Corp., Norwalk, CT) with a volume of 50 μL containing 200 μM each dNTP, 0.3 μM each primer, 1 ng of template pBDHVU1, 1.5 mM $MgCl_2$ in Expand HF buffer (as supplied by the manufacturer), and 1.3 units of enzyme mix (*Taq* DNA and *Pwo* DNA polymerases). The cDNA coding for the C-terminal domain of BDH was amplified in 35 cycles consisting of 0.5 min at 94 °C, 1 min at 65 °C, and 1 min at 72 °C, followed by 10 min at 72 °C. The 327 bp fragment produced by PCR was doubly digested with *Bam*HI and *Eco*RI and then ligated to the pBluescript SK(−) vector (Stratagene, La Jolla, CA) for DNA sequencing. No error was detected as compared with the original HH-BDH sequence. The cDNA fragment was excised from pBluescript with *Bam*HI and *Eco*RI and subcloned into the corresponding sites in the vector pGEX2T for expression in *Escherichia coli* [strain BL21(DE3)]. This plasmid (pGSTCTB1) codes for the GST-CTBDH fusion protein (calculated M_r of 38 259) which contains three parts, GST, a peptide linker (SDLVPRGS) including a thrombin cleavage site, and CTBDH (residues 195−297 of HH-BDH) (Figure 1). In this construct, CTBDH lacks one residue (N194) of the previously defined C-terminal domain of HH-BDH [residues 194−297, adjacent to the last residue of HH-BDH (G193) conserved in the SC-ADH (*10*)].

Expression and Purification of GST-CTBDH. LB medium (500 mL) containing ampicillin (150 μg/mL) was inoculated with an overnight culture (10 mL) of pGSTCTB1 in BL21(DE3) and incubated with shaking at 30 °C. At an OD_{600nm} of 0.8, IPTG was added to a final concentration of 0.1 mM, and after an additional 3 h incubation, the bacteria were harvested [centrifugation in a JA-10 rotor (Beckman Corp., Fullerton, CA) at 7000 rpm for 10 min at 4 °C]. The bacterial pellet was resuspended in STE buffer [10 mM Tris-HCl (pH 8.0), 150 mM NaCl, 1 mM EDTA], respun, and then frozen at −80 °C. After being thawed, the bacterial pellet was resuspended in 30 mL of STE buffer containing 5 mM DTT, and the sample was adjusted to 1.5% *N*-lauroylsarcosine (Sigma Chemical Co., St. Louis, MO) added from a 15% stock solution. The bacteria were then lyzed using a French pressure cell (two passes at ∼10 000 psi). The lysate was treated with pancreatic ribonuclease A and deoxyribonuclease I (each at a final concentration of 10 μg/mL) and incubated on ice for 10 min. Then PMSF was added (final concentration of 1 mM), and the solution was clarified by centrifugation [JA-20 rotor (Beckman Corp., Fullerton, CA) at 20 000 rpm for 20 min at 4 °C]. After centrifugation, the insoluble fraction in the pellet (taken up in 30 mL of 6 M urea) and the supernatant were analyzed by SDS−PAGE. The supernatant fraction (∼30 mL) was added to 2 mL of glutathione−Sepharose 6B beads (Pharmacia Biotech, Piscataway, NJ) and mixed gently for 1 h at 4 °C on a rotating arm. After binding, the beads were washed two times with 20 mL of PBS buffer [140 mM NaCl, 2.7 mM KCl, 10 mM Na_2HPO_4, 1.8 mM KH_2PO_4 (pH 7.3)], and then purified GST-CTBDH was recovered using 6 mL of elution buffer [50 mM Tris-HCl (pH 8.0), 5 mM DTT, 150 mM NaCl, 1% octyl glucoside with 10 mM reduced glutathione]. The fusion protein (at a concentration of <1 mg/mL) was dialyzed against 10 mM Hepes−NaOH (pH 7.0) with 0.2 M NaCl and 10 mM DTT and then quick-frozen in liquid nitrogen and stored at −80 °C. The residual octyl glucoside concentration after dialysis was <0.04% as quantitated by the anthrone assay for glucose (*21*).

Expression and Purification of Recombinant GST. GST (calculated M_r of 26 986) was expressed from the pGEX2T vector and purified as described by Pharmacia Biotech (Piscataway, NJ). This form of GST (from *Schistosoma japonicum*) is expressed with 14 additional C-terminal residues with the sequence SDLVPRGSPGIHRD, extending beyond the natural C-terminus of this enzyme (...HPPK; see Figure 1).

Immunoblotting. Samples were separated by SDS−PAGE with 12% acrylamide gel (*22*) and transferred as described previously (*17*) to a poly(vinylidene difluoride) membrane (PVDF, Immobilon-P, 0.45 μm; Millipore, Bedford, MA). Immunodetection was performed essentially as described (*17*) using either anti-BDH rabbit antibody (*10*) (dilution 1:100) or anti-GST goat antibody (dilution 1:500) followed by alkaline phosphatase conjugated antibody (either anti-rabbit or anti-goat, respectively) treatment and color reaction.

Preparation of Phospholipid Vesicles. PC or DGDG vesicles (100 μg of phosphorus/mL or 3 mM) were prepared in 20 mM Hepes−NaOH (pH 8.0) with 1 mM EDTA (buffer B) using the sonication procedure described in Cortese et al. (*23*). The PE/DPG vesicles were prepared by mixing PE and DPG (at a 9 to 1 molar ratio) in organic solvent prior to drying, hydration, and sonication. [^{3}H]PC (1-palmitoyl-2-oleoyl-[9,10-^{3}H]glycero-3-phosphocholine) was prepared as described by Eibl et al. (*24*) and with a specific radioactivity of 3.7 μCi/μmol (stock solution concentration of 8 mM). To prepare [^{3}H]PC-labeled PC vesicles, [^{3}H]PC (32 nmol, ∼2.6 × 10^5 dpm) was evaporated under nitrogen and 250 μL of PC (3.2 mM in buffer B) was added. The solution was mixed vigorously using a vortex mixer, then sonicated, and filtered through a 0.22 μm GSTF filter (Millipore, Bedford, MA). For preparation of DGDG vesicles containing [^{3}H]PC as tracer, [^{3}H]PC stock solution (0.13 μmol, ∼1.1 × 10^6 dpm) and DGDG (3.2 μmol) were dried together from organic solvent. Buffer B (1 mL) was added, and the lipids were dispersed by sonication followed by filtration through a 0.22 μm GSTF filter. Lipid vesicles containing various concentrations of pyrenyl-PC or pyrenyl-PE were prepared by mixing aliquots of PE (11.25 μg of phosphorus) and DPG (1.25 μg of phosphorus) plus the desired amount of an equimolar mixture of either pyrenyl-PC and dioleoyl-PC (pyrenyl-PC concentration of 0.05% to 25% of total lipid phosphorus) or of pyrenyl-PE and dioleoyl-PE (with pyrenyl-PE up to 10% of the total lipid phosphorus). The phospholipid mixtures in organic solvent (chloroform/methanol, 2/1) were dried and dispersed by sonication in 500 μL of buffer B. The pyrenyl-PC content of the lipid vesicles in the range from 2.5% to 25% pyrenyl-PC was confirmed from the absorption spectra.

Flotation in Sucrose Density Gradients. HH-Histag-BDH or GST-CTBDH (40 μg) was incubated at room temperature with either PC, DGDG, or PE/DPG vesicles at a ratio of

200 mol of lipid/mol of protein in buffer B and 5 mM DTT. HH-Histag-BDH−lipid samples also contained 5 mM NAD^+. The final volumes of the mixtures were 100 μL for HH-Histag-BDH and 120 μL for GST-CTBDH, with NaCl of either 10 or 70 mM, respectively (derived from the protein stock solutions). After 30 min incubation, each sample was applied directly to the sucrose gradient or additional NaCl (4 M) was added to a final concentration of 0.5 M. Then the samples were adjusted to 30% sucrose (by addition of 50% sucrose) and placed at the bottom of an ultracentrifuge tube over a cushion of 40% sucrose. The volume of the cushion was adjusted to give a total volume of 0.45 mL (for cushion plus sample). All sucrose solutions were prepared in HDN buffer [5 mM Hepes−NaOH (pH 8.0) containing 2 mM DTT and 0.1 M NaCl]. Each sample was overlaid with a discontinuous sucrose gradient (1 mL of 25% sucrose, 0.5 mL of 5% sucrose, and 0.25 mL of HDN buffer) and centrifuged (50 000 rpm for 16 h at 4 °C) in a TLS 55 rotor (Beckman Corp., Fullerton, CA). Fractions (200 μL) were collected from the top, and aliquots (20 μL) of each fraction were analyzed by SDS−PAGE on precast 12% acrylamide gels (FMC Bioproducts, Rockland, ME). The concentration of sucrose in each fraction was measured using a refractometer (Bausch & Lomb, Rochester, NY).

For GST-CTBDH, the same experiment was repeated except using either PC vesicles or DGDG vesicles, each containing [^{3}H]PC as tracer. Aliquots (30 μL) of each sucrose gradient fraction were mixed with 4.5 mL of scintillation liquid (Cytoscint, ICN Pharmaceuticals, Costa Mesa, CA), and radioactivity was counted in a Beckman LS 5000TD counter. The lipid/protein mole ratios in each fraction were calculated from the measured radioactivity for the lipid and the percentage of protein found in each fraction (as determined by densitometry and assuming 100% recovery of protein from the gradient).

Tryptophan Fluorescence Quenching. HH-Histag-BDH, GST, CTBDH, and GST-CTBDH have five, four, three, and seven tryptophan residues, respectively. Either GST-CTBDH or Histag-BDH (3 μg) (or GST for control) was reconstituted at room temperature with phospholipid vesicles containing either pyrenyl-PC (from 0% to 25% of total phosphorus) with a constant background of PE/DPG (0.225 and 0.025 μg of phosphorus, respectively) or pyrenyl-PE (0−10% of total phosphorus) with a constant background of PC/DPG (0.225 and 0.025 μg of phosphorus, respectively) each in buffer B with 5 mM DTT (final volume: 300 μL). After 1 h incubation at room temperature (23 °C), the absorbance and fluorescence of each sample were measured. The absorbance readings were taken on a Shimadzu (Columbia, MD) Model UV-2501PC spectrophotometer. Fluorescence measurements were performed essentially as described previously (*6*) at room temperature using a Perkin-Elmer MPF-44B fluorometer (Norwalk, CT) in the ratio mode, with 4 × 4 mm pathlengh cuvettes (excitation at 290 nm and emission at 340 nm, 12 and 10 or 20 nm slit widths, respectively). Fluorescence values were corrected for inner filter effects as described by Lakowicz (*25*), i.e., multiplying the measured fluorescence by the factor [antilog(absorbance at 290 nm + absorbance at 340 nm)/2]. Inner filter effects were significant only for samples with >10% pyrenyl-PC. The data were normalized to the fluorescence of each protein reconstituted into PC/PE/DPG vesicles in the absence of pyrenyl-PC or pyrenyl-PE [relative tryptophan fluorescence intensities were 600, 462, and 284 (arbitrary units) for HH-Histag-BDH, GST-CTBDH, and GST, respectively]. For HH-Histag-BDH and GST-CTBDH reconstituted into PE/DPG vesicles, the fluorescence intensities were ∼10% lower than in PC/PE/DPG vesicles with 50% dioleoyl-PC. Fluorescence quenching data were plotted according to the Stern−Volmer equation (*25*) (F_0/F versus pyrenyl-PC) or according to Lehrer (*26*) [$F_0/(F_0 - F)$ versus either 1/pyrenyl-PC or 1/pyrenyl-PE], where F_0 and F are the fluorescence intensities in the absence and presence of pyrenyl-PC or pyrenyl-PE. The Lehrer plots of the quenching by pyrenyl-PE were linear, and those with pyrenyl-PC were biphasic; quenching parameters were determined by linear regression analysis of each segment to obtain the fraction of fluorescence accessible to the quencher, $(f_a)_{eff}$ (from the reciprocal of the *y*-intercept) and the effective Stern−Volmer quenching constant, $(K_Q)_{eff}$ (from the *y*-intercept/slope), expressed as the reciprocal concentration of pyrenyl-PC or pyrenyl-PE quencher in the lipid vesicles, i.e., $(\%)^{-1}$.

Thrombin Digestion. GST-CTBDH (1 mg/mL) was incubated in 10 mM Hepes−NaOH (pH 7.3), 0.2 M NaCl, and 10 mM DTT at room temperature with thrombin (100 units/mg of GST-CTBDH). After 2 h, 4× gel loading mix [to give a final concentration of 10% (v/v) glycerol, 2% (w/v) SDS, 1.25% (v/v) β-mercaptoethanol in 60 mM Tris-HCl (pH 6.8)] was added to inactivate the thrombin. Digested GST-CTBDH (5 μg) was analyzed by SDS−PAGE on a precast 4−20% acrylamide gel (Bio-Rad Corp., Hercules, CA) stained with Coomassie Blue. For time course digestion of GST-CTBDH in the presence versus absence of PC, a similar procedure was used except that GST-CTBDH (0.2 mg/mL) was preincubated for 30 min at room temperature in buffer B containing 10 mM DTT either without or with PC vesicles (lipid/protein mole ratio of 200) prior to addition of thrombin. The digestion time course (up to 20 h digestion) was quantitated by scanning densitometry of the remaining GST-CTBDH in SDS−PAGE stained with Coomassie Blue. Digital images of gels were obtained with a HP 6100P scanner (Hewlett-Packard, Palo Alto, CA) and Visioneer PaperPort 3.0.1 software (Visioneer Communications, Inc., Palo Alto, CA). Densitometry was carried out using the DNA ProScan A13 software (Technology Resources, Nashville, TN).

For sucrose gradient fractionation of GST-CTBDH cleaved by thrombin, a modification of the sucrose gradient method described above was used. GST-CTBDH was preincubated with PC vesicles for 30 min at room temperature, and then thrombin (100 units/mg of GST-CTBDH) was added. The mixture was incubated for an additional 2 h at room temperature to achieve close to complete cleavage of GST-CTBDH. After centrifugation in a sucrose step gradient (see above), fractions were analyzed either by SDS−PAGE on precast 12% acrylamide gels (FMC BioProducts, Rockland, ME) stained with Coomassie Blue (20 μL aliquots) or by Western blot analysis (15 μL aliquots) using 16% acrylamide gels followed by detection with anti-BDH antiserum.

Mass Spectrometry Analysis of CTBDH. GST-CTBDH (40 μg) was digested by thrombin for 2 h as described above. The reaction mixture was loaded on a Sep-Pak C18 cartridge (Waters, Milford, MA), which was then washed with 0.1% TFA. The products of thrombin digestion were eluted with

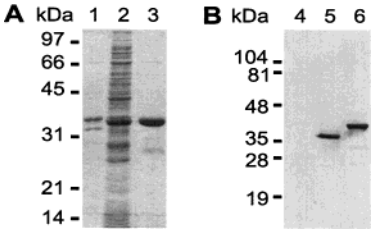

FIGURE 2: Purification of GST-CTBDH (panel A) and reaction with anti-BDH antibody (panel B). Panel A: GST-CTBDH was expressed in *E. coli*, solubilized by lysis in 1.5% *N*-lauroylsarcosine, and centrifuged (see Experimental Procedures) to obtain a pellet (insoluble fraction, taken up in 6 M urea, lane 1) and supernatant (lane 2) which were analyzed by SDS−PAGE (12% acrylamide gel, Coomassie Blue stain), loading the equivalent of 2 μL of lysate per lane. Purified GST-CTBDH after dialysis (see Experimental Procedures) is shown in lane 3 (2 μg of protein). Panel B: Reaction of GST-CTBDH with anti-BDH antibody. Samples (0.5 μg of protein each) of GST (lane 4), HH-Histag-BDH (lane 5), and purified GST-CTBDH (lane 6) were analyzed by Western blot using anti-BDH polyclonal antibody (see Experimental Procedures). For both panels A and B, positions of molecular size markers are shown at the left.

acetonitrile/0.1% TFA (6/4), concentrated under vacuum, and analyzed by MALDI (matrix-assisted laser desorption ionization) mass spectrometry (*28*). Sinipanic acid [10 mg/mL in acetonitrile/0.1% TFA (7/3)] was used as an additive matrix and cytochrome *c* as an internal standard (stock solution of 5 pmol/μL). Samples for mass spectrometry analysis were prepared as follows: 2 μL of sample was mixed with standard cytochrome *c* and 4 μL of sinipanic acid matrix solution. Aliquots (2 μL each) of this mixture were deposited onto a sample plate and allowed to dry prior to mass analysis. Mass spectrometry was carried out on a Voyager Elite MALDI time-of-flight mass spectrometer (PerSeptive Biosystems, Framingham, Boston, MA) at an accelerating voltage of 25 keV in the linear delayed-extraction positive ion mode. The accuracy of the measurements given by the manufacturer is 0.02%. The instrument was calibrated internally with cytochrome *c* using $[M + H]^+ = 12361.1$ and $[M + 2H]^{2+} = 6181$.

RESULTS

GST-CTBDH Expression and Purification. The cDNA encoding the C-terminal domain of HH-BDH (residues 195−297) was ligated into an expression plasmid so as to produce a novel fusion protein, GST-CTBDH, in which CTBDH is located at the C-terminus of GST (Figure 1). GST-CTBDH includes a linking peptide (SDLVPRGS) that provides a thrombin cleavage site between the GST and CTBDH domains (Figure 1). The fusion protein that is expressed in *E. coli* can be almost completely solubilized in the bacterial lysate using 1.5% *N*-lauroylsarcosine (Figure 2A, lane 2). Under these conditions, little urea-soluble protein remained in the pellet (Figure 2A, lane 1). Other detergents such as 1% Triton X-100, 1% CHAPS, 1% sodium cholate, or 60 mM octyl glucoside failed to solubilize GST-CTBDH as determined by SDS−PAGE (not shown). From the 1.5% *N*-lauroylsarcosine lysate, GST-CTBDH could be purified in one step by affinity chromatography using a glutathione−Sepharose matrix (Figure 2A). Typically 60% of GST-CTBDH bound to the matrix as estimated from the GST activity in the lysate versus the effluent. GST-CTBDH was eluted from the glutathione−Sepharose with glutathione in 1% octyl glucoside (~60% recovery based on GST activity), yielding a highly purified protein preparation (Figure 2A, lane 3) (~10 mg/L bacterial culture, recovering 30−40% of the GST activity measured in the lysate). The addition of either 2% or 4% Triton X-100 to the 1.5% *N*-lauroylsarcosine supernatant did not affect the yield of purified GST-CTBDH (not shown) although 1% octyl glucoside in the eluent was required for optimal recovery of GST-CTBDH. After dialysis to remove octyl glucoside, GST-CTBDH remains soluble up to ~1 mg/mL. The residual detergent concentration was <0.04% as measured by the anthrone assay for glucose (*21*). The fusion protein has an apparent size of 37 kDa (by comparison with protein standards on SDS−PAGE) whereas GST alone is 28 kDa. Reaction with polyclonal anti-BDH antibody (Figure 2B, lane 6) confirms the presence of BDH epitope(s) in GST-CTBDH which also reacts with anti-GST antibodies (not shown). GST-CTBDH has a glutathione transferase specific activity of ~160 units/μmol, about 2-fold lower than the specific activity of recombinant GST (320 units/μmol). Thus, the purified recombinant fusion protein is immunoreactive to both GST and BDH antibodies and contains a catalytically active GST domain consistent with properties expected for GST-CTBDH.

Lipid Vesicle Binding Selectivity of HH-Histag-BDH and GST-CTBDH. The binding of HH-Histag-BDH and GST-CTBDH to either PC or DGDG vesicles was characterized and quantitated by flotation in sucrose density gradients (Figure 3) measuring the distribution of both protein (by SDS−PAGE) and lipid (by radioactivity as depicted in the histograms). For HH-Histag-BDH preincubated with PC vesicles (Figure 3A, upper panel), most of the protein (~90% by scanning densitometry, not shown) after sucrose gradient fractionation was near the top (fractions 2−6), consistent with almost quantitative binding of HH-Histag-BDH to the PC vesicles. A small fraction of the protein (~10%) remained near the bottom (fractions 10 and 11). Similar results were found with GST-CTBDH with essentially all the protein floating to near the top of the sucrose gradient (fractions 2−5) (Figure 3A). In the absence of PC vesicles, both proteins remained at the bottom of the gradient (not shown). In the absence of protein, [^{3}H]PC vesicles migrated near the top of the gradient (fraction 1) with decreasing concentrations in fractions 2 and 3 (open bars, Figure 3A). For the fractionated GST-CTBDH complex with PC vesicles, the lipid distribution (Figure 3A, upper panel histogram) is similar to the protein distribution, with the highest concentration of PC being found in fraction 3 that also contained the peak protein (50%). For the GST-CTBDH complex with PC, the calculated lipid/protein mole ratios in fractions 2, 3, and 4 (totaling 96% of recovered protein) were 515, 137, and 81, respectively, with an average L/P ratio of 166 (in fractions 2−4 combined) that is not significantly different from the initial L/P ratio of 200, considering that ~10% of the lipid (fraction 1) is devoid of detectable protein. After fractionation of HH-Histag-BDH reconstituted with PC vesicles, the PC distribution was found to be similar (not shown) to the HH-Histag-BDH protein that is distributed in fractions 2−5 of the gradient. For either GST-CTBDH or HH-Histag-BDH reconstituted with PC-vesicles, treatment with either 0.5 M NaCl or 0.4 M LiBr prior to sucrose gradient centrifugation did not affect the protein or lipid distribution. By contrast,

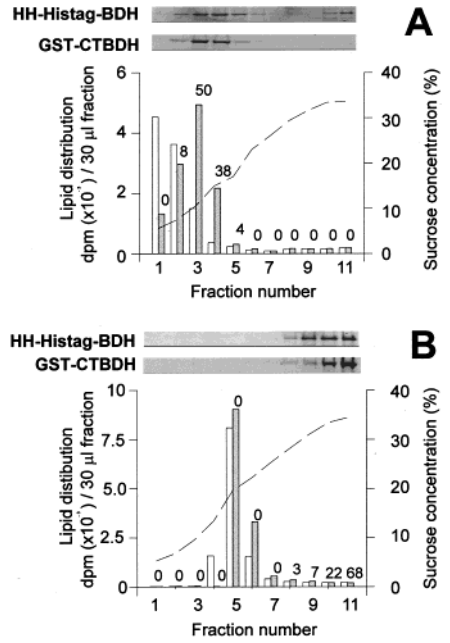

FIGURE 3: Selective binding of HH-Histag-BDH and GST-CTBDH to PC vesicles versus DGDG vesicles. HH-Histag-BDH (0.4 mg/mL) or GST-CTBDH (0.33 mg/mL) was incubated (30 min at room temperature) with PC vesicles (panel A) or DGDG vesicles (panel B) at a lipid/protein molar ratio of 200. After addition of NaCl to 0.5 M, the samples were separated by 16 h centrifugation over discontinuous sucrose gradients in 5 mM Hepes−NaOH (pH 8.0), 2 mM DTT, and 0.1 M NaCl (see Experimental Procedures). Fractions (200 μL) collected from the top of each tube (samples 1−11, top to bottom of gradient) were analyzed by SDS−PAGE with Coomassie Blue staining. For each fraction, only the band corresponding with the appropriate protein is shown (35 kDa for HH-Histag-BDH and 37 kDa for GST-CTBDH), no other protein bands being detected. The histograms depict the distribution in the sucrose gradients of either PC (panel A) or DGDG (panel B) vesicles (each with [^{3}H]PC as a tracer) after preincubation in either the absence (open bars) or presence (gray bars) of GST-CTBDH. The numbers above the gray bars are the relative amount of GST-CTBDH in each fraction (expressed as percent of total) as determined by scanning densitometry of the SDS−PAGE gels of GST-CTBDH. The sucrose concentration profile is also shown (− −). Each result shown is typical of at least two independent experiments.

after preincubation of either HH-Histag-BDH or GST-CTBDH with DGDG vesicles (a bilayer-forming lipid that does not activate BDH), essentially all of the protein remained near the bottom of the gradient (>95% in fractions 9−11) (Figure 3B, lower panels), indicating that neither of these proteins formed a complex with DGDG. This is confirmed by the distribution of the DGDG vesicles in the fractionated sucrose gradients. The DGDG vesicles alone appear to be somewhat more dense than PC vesicles, with DGDG distributing around fraction 5 (14−22% sucrose fractions, Figure 3B) with a mean density of 1.07 g/mL as compared with PC vesicles that float near the top of the gradient (5−11% sucrose, Figure 3A) with a density of ~1.03 g/mL. However, the DGDG distribution was essentially unchanged after preincubation with either GST-CTBDH (Figure 3B, lower panel histogram) or HH-Histag-BDH (not shown), with the lipid being separated from the protein. Thus, neither GST-CTBDH nor HH-Histag-BDH form a complex with DGDG (Figure 3B) under conditions where both of these proteins form salt-stable complexes with PC vesicles (Figure 3A).

After reconstitution with PE/DPG vesicles, HH-Histag-BDH and GST-CTBDH were each found to float in the sucrose gradients (not shown), indicating formation of complexes of each protein with PE/DPG vesicles analogous to the complexes formed with PC vesicles (see Figure 3A, upper panel). However, after treatment with either 0.4 M NaCl or 0.4 M LiBr, both HH-Histag-BDH and GST-CTBDH that had each been reconstituted with PE/DPG vesicles yielded results similar to those with DGDG vesicles (not shown), consistent with salt-induced dissociation of these two protein−PE/DPG complexes. In these studies, it was noted that, after the addition of either 0.4 M NaCl or 0.4 M LiBr to PE/DPG samples (in either the presence or absence of protein), the solutions became cloudy, suggesting a salt-induced change in the bulk properties of the PE/DPG that was not evident in the studies with either PC or DGDG vesicles. In control studies, GST, preincubated with either PC, PE/DPG, or DGDG vesicles, remained near the bottom of the gradients, consistent with lack of GST binding to these lipids (not shown). In summary, these studies show that GST-CTBDH and HH-Histag-BDH each form salt-stable complexes with PC vesicles and salt-dissociable complexes with PE/DPG vesicles but do not bind to DGDG vesicles. Therefore, both proteins exhibit a similar PC-selective binding to lipid vesicles.

Binding of Pyrenyl-PC or Pyrenyl-PE to HH-Histag-BDH or GST-CTBDH Quantitated by Quenching of Tryptophan Fluorescence. The fluorescent phospholipid, pyrenyl-PC, has been shown to activate bovine heart BDH and to quench its tryptophan fluorescence (*6*). Reconstitution of either HH-Histag-BDH or GST-CTBDH into phospholipid vesicles with increasing pyrenyl-PC content results in a progressive and marked quenching of fluorescence (Figure 4A). The quenching profile is distinctly biphasic with >30% quenching being effected by pyrenyl-PC concentrations up to ~1% of the total lipid with only an additional 10−20% quenching being observed as the pyrenyl-PC is increased to 10% with no additional quenching at up to 25% pyrenyl-PC in the lipid vesicles. Control samples, prepared by reconstituting either HH-Histag-BDH or GST-CTBDH into phospholipid vesicles without pyrenyl-PC but containing 50% dioleoyl-PC, exhibited a slight increase in fluorescence (~10%) compared with the same proteins in PE/DPG vesicles devoid of PC. A set of controls with GST alone, titrated with phospholipid vesicles containing up to 25% pyrenyl-PC, exhibited an essentially constant tryptophan fluorescence [F_0 of 284 arbitrary units, SEM of ±6% (n = 14)] (not shown). By contrast with the efficient quenching observed with pyrenyl-PC in PE/DPG vesicles (Figure 4A), the tryptophan fluorescence of control samples of either HH-Histag-BDH or GST-CTBDH, reconstituted into PC/DPG vesicles containing pyrenyl-PC (1%), was quenched by only ~10% (not shown). Thus, the initial phase of the tryptophan fluorescence quenching by pyrenyl-PC in the PE/DPG background (Figure 4A) is not observed in the presence of an excess of PC and appears to reflect the specificity of each of these proteins for PC. For HH-Histag-BDH or GST-CTBDH in PE/DPG and titrated with pyrenyl-PC, Stern−Volmer plots of the tryptophan fluorescence quenching were nonlinear (not shown), and Lehrer plots (inset Figure 4A) are distinctly biphasic. At low pyrenyl-PC concentrations (up to ~2.5% pyrenyl-PC), a linear Lehrer plot is observed for both HH-

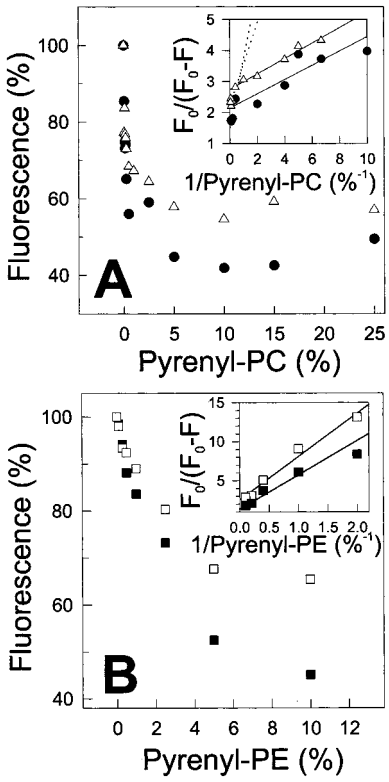

FIGURE 4: Quenching of HH-Histag-BDH and GST-CTBDH tryptophan fluorescence by either pyrenyl-PC (panel A) or pyrenyl-PE (panel B) in lipid vesicles. Panel A: Aliquots (3 μg) of either HH-Histag-BDH (△) or GST-CTBDH (●) were reconstituted into lipid vesicles with pyrenyl-PC content, as indicated, in 20 mM Hepes−NaOH (pH 8.0), 1 mM EDTA, and 5 mM DTT at ambient temperature (~23 °C). Tryptophan fluorescence was measured (excitation at 290 nm, emission at 340 nm) and corrected for inner filter effects (see Experimental Procedures). The data are normalized to the fluorescence of each protein reconstituted into PC/PE/DPG (50% dioleoyl-PC) vesicles without pyrenyl-PC [600 and 462 (arbitrary units) for HH-Histag-BDH and GST-CTBDH, respectively] and are the mean of three or two independent experiments with average SEM of ±15% and ±18% for the individual data points for HH-Histag-BDH and GST-CTBDH, respectively. The inset in panel A is a Lehrer plot (*26*) of the same data (values for <0.1% pyrenyl-PC are not shown). The parameters calculated for the two components of the quenching (solid and dotted lines in the inset) are given in Table 1. Panel B. As in (A), except that HH-Histag-BDH (□) or GST-CTBDH (■) was reconstituted into lipid vesicles with pyrenyl-PE content as indicated. Data plotted are the mean of three independent determinations with average SEM of ±10% and ±12% for the individual data points for HH-Histag-BDH and GST-CTBDH, respectively. The inset in panel B is a Lehrer plot of the same data with calculated parameters given in Table 1.

Histag-BDH or GST-CTBDH. In this range of pyrenyl-PC concentrations, the fraction of quenchable fluorescence, $(f_a)_{eff}$, is similar for the two proteins, and the effective Stern−Volmer quenching constants $(K_Q)_{eff}$ are the same within error (Table 1). Although the two proteins have somewhat different initial tryptophan fluorescence intensities (F_0 of 600 and 462 arbitrary units for HH-Histag-BDH and GST-CTBDH, respectively), the fluorescence signal that is quenchable by low pyrenyl-PC concentrations is similar for both proteins [216 and 217 arbitrary units, respectively, as calculated from F_0 and $(f_a)_{eff}$ values] and consistent with quenching of the tryptophans in the CTBDH domain of each protein. For the low (<2.5%) pyrenyl-PC range, the reciprocal of $(K_Q)_{eff}$ approximates 0.1% pyrenyl-PC and is equivalent to the concentration of the quencher in the lipid vesicle bilayer at which 50% of the accessible fluorescence is quenched (*25*, *26*). For both HH-Histag-BDH and GST-CTBDH, the tryptophan fluorescence quenching afforded by low pyrenyl-PC concentrations is in the range for stoichiometric interaction of pyrenyl-PC with the protein. At higher pyrenyl-PC concentrations (>2.5%), a second component of quenching is observed with a $(K_Q)_{eff}$ approximately an order of magnitude lower than for quenching by low pyrenyl-PC and resulting in a further reduction in fluorescence, calculated to be about 9% and 19% for HH-Histag-BDH and GST-CTBDH, respectively.

Table 1: Parameters of Tryptophan Fluorescence Quenching by Pyrenyl-PC or Pyrenyl-PE for HH-Histag-BDH and GST-CTBDH[a]

phospholipid	HH-Histag-BDH	GST-CTBDH
low pyrenyl-PC		
$(f_a)_{eff}$	0.36	0.47
$(K_a)_{eff}$ (%)$^{-1}$	11	9.3
high pyrenyl-PC		
$(f_a)_{eff}$	0.45	0.66
$(K_Q)_{eff}$ (%)$^{-1}$	1.7	0.68
pyrenyl-PE		
$(f_a)_{eff}$	0.46	0.72
$(K_Q)_{eff}$ (%)$^{-1}$	0.36	0.29

[a] For HH-Histag-BDH and GST-CTBDH, the quenching of tryptophan fluorescence by pyrenyl-PC or pyrenyl-PE, plotted according to Lehrer (*26*) (see insets in Figure 4), was analyzed by linear regression for low pyrenyl-PC (≤2.5%, solid lines, Figure 4A) or high pyrenyl-PC (≥2.5%, dashed lines, Figure 4A) corresponding to the two segments of the biphasic quenching or for the complete range of pyrenyl-PE tested (up to 10%, Figure 4B). For each range of pyrenyl-PC or pyrenyl-PE concentrations, the values for $(f_a)_{eff}$, the effective fractional accessible fluorescence, and $(K_Q)_{eff}$, the effective Stern−Volmer quenching constant, were calculated as described in Experimental Procedures. Correlation coefficients were 0.98, 0.71, and 0.99 for HH-Histag-BDH and 0.95, 0.92, and 0.97 for GST-CTBDH (low pyrenyl-PC, high pyrenyl-PC, and pyrenyl-PE, respectively).

Titration of either HH-Histag-BDH or GST-CTBDH with pyrenyl-PE (Figure 4B) also quenches a total fraction of the tryptophan fluorescence of either protein similar to that quenched by titration with pyrenyl-PC (Figure 4A) but with effective Stern−Volmer quenching constants more than an order of magnitude lower than for pyrenyl-PC (Table 1). With pyrenyl-PE, the $(K_Q)_{eff}$ values are comparable to those for the lower affinity second component of quenching observed with the higher concentrations of pyrenyl-PC. With pyrenyl-PE, half-maximal quenching is obtained at ~3% pyrenyl-PE in the lipid bilayer for both HH-Histag-BDH and GST-CTBDH. For both proteins, pyrenyl-PC or pyrenyl-PE quench a similar fraction of the tryptophan fluorescence (Figure 4 and Table 1). An appreciable fraction of the fluorescence (i.e., ~55% for HH-Histag-BDH and ~40% for GST-CTBDH) is not quenched even by the highest concentrations of pyrenyl-PC or pyrenyl-PE tested and is likely referable to one or more of the tryptophans located in the aqueous domain of each molecule (two in BDH and four in GST). For the fluorescence that is quenchable by pyrenyl-PC or pyrenyl-PE, the quenching parameters are similar for the two proteins, HH-Histag-BDH and GST-CTBDH, though different for the two lipids (PC versus PE).

Thrombin Digestion of GST-CTBDH. Digestion of GST-CTBDH with thrombin yielded two fragments detected by SDS−PAGE (Figure 5A, lane 2), one of ~26 kDa (similar to the calculated size for GST, 27 kDa) and the second,

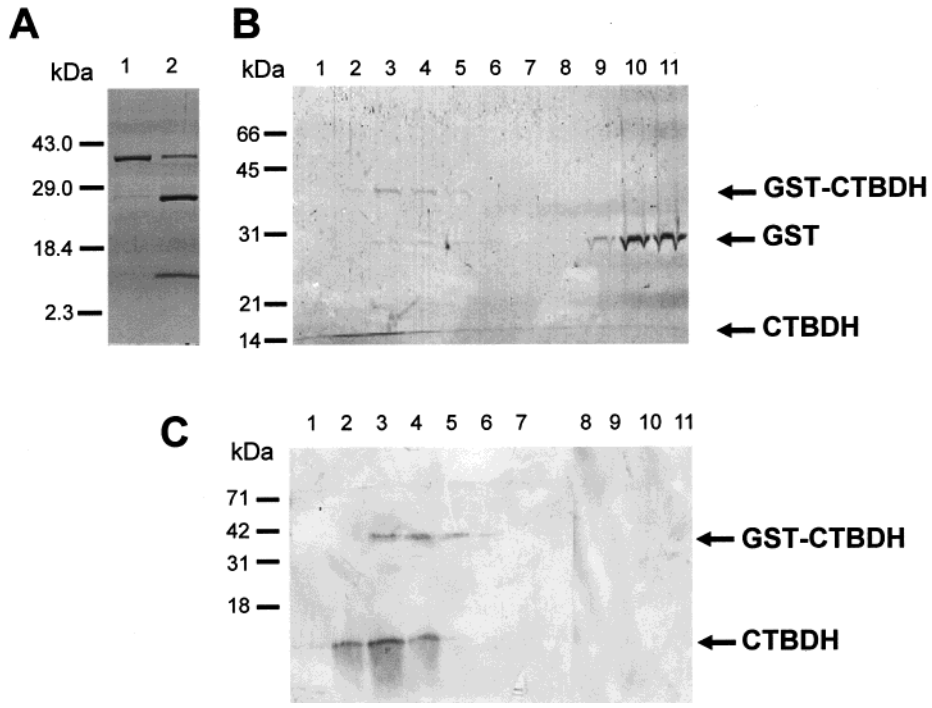

FIGURE 5: CTBDH peptide, obtained by thrombin cleavage of GST-CTBDH, remains bound to PC vesicles. Panel A: GST-CTBDH was incubated with thrombin for 2 h at room temperature and analyzed by SDS−PAGE (4−20% gradient gel) stained with Coomassie Blue (lanes 1 and 2 are GST-CTBDH before and after 2 h cleavage, 1.5 and 5 μg of protein, respectively). Panels B and C: GST-CTBDH, preincubated with PC vesicles (200 mol of PC/mol of GST-CTBDH), was cleaved (2 h) with thrombin and, after addition of 0.5 M NaCl, was fractionated over a sucrose gradient (see Figure 3). After centrifugation, fractions (200 μL) were collected from the top (fraction 1) of each tube, and 20 μL of each fraction was analyzed either by SDS−PAGE (12% polyacrylamide) stained with Coomassie Blue (panel B) or by Western blot (16% polyacrylamide) using anti-BDH serum (panel C). Positions of protein bands corresponding with GST-CTBDH, GST, and CTBDH are identified.

referable to CTBDH, with an estimated size of ~7.8 kDa (by comparison with protein standards on SDS−PAGE). The apparent size of CTBDH by SDS−PAGE was 1.6-fold lower than the theoretical value, based on the amino acid sequence (12 111 Da). Mass spectrometric analysis of GST-CTBDH digested by thrombin showed two ions (m/z = 6056.9 and 12 111.8) (spectra not shown) that correspond to different protonated states (2 and 1, respectively) yielding an average molecular mass of 12 111.3 Da. Three independent sample analyses (total of four determinations) gave a molecular mass of 12 111.1 ± 0.4 Da for the single protonated species. This mass is the same as the predicted size of the C-terminal fragment (CTBDH) obtained via thrombin-specific cleavage of GST-CTBDH. The smaller size of CTBDH measured by SDS−PAGE indicates that this protein runs anomalously fast in the electrophoresis system. The half-time for thrombin digestion of GST-CTBDH was ~1 h, and complete cleavage of GST-CTBDH was achieved after 20 h of digestion (not shown). The rate of cleavage of GST-CTBDH by thrombin, as quantitated by densitometry, was similar whether or not GST-CTBDH had been reconstituted with PC vesicles (not shown), indicating that thrombin cleavage of the fusion protein is not affected by the PC bilayer.

Sucrose gradient flotation studies of GST-CTBDH cleaved by thrombin (after reconstitution with PC vesicles) show that the smaller peptide, CTBDH, floated with PC vesicles as detected by both Coomassie staining (at the dye front in Figure 5B) and Western blot (Figure 5C), while the GST fragment remained near the bottom of the gradient (Figure 5B). Since the thrombin digestion was incomplete after 2 h (~35% remaining GST-CTBDH), the residual GST-CTBDH is also detected by SDS−PAGE (Figure 5B) and Western blot (Figure 5C) in the upper part of the gradient (lower density fractions, 3−5), consistent with GST-CTBDH also remaining complexed with PC vesicles (see Figure 3A). Similar results were obtained with CTBDH prepared from GST-CTBDH by digestion with thrombin prior to incubation with PC vesicles (not shown). Thus, CTBDH formed by cleavage of GST-CTBDH binds to PC vesicles, reflecting an intrinsic PC binding property of this domain of BDH.

DISCUSSION

BDH is a PC-dependent lipid-requiring enzyme in which the C-terminal third of the 297-residue sequence was postulated to form a domain containing elements that determine substrate specificity and/or form the PC binding site of the protein (*10*). Recent computerized searches of the protein databases reaffirm that BDH is a SC-ADH and identify the human 17β-hydroxysteroid dehydrogenases (types 1, 2, and 3, each in the SC-ADH family) among proteins with the highest sequence homology to human heart BDH. These database searches confirm the unique character of the C-terminal segment of BDH in that this part of the protein has limited sequence homology with the SC-ADH or any other protein (not shown). For example, the type 2 human 17β-hydroxysteroid dehydrogenase (*29*) has 33% overall identity to HH-BDH, with ~40% identity in the N-terminal two-thirds of their sequences (corresponding to the NADH and catalytic domains) but only 23% identity in their C-terminal segments (not shown). In the studies reported here, the C-terminal domain (residues 195−297) of HH-BDH has now been expressed as a chimera with GST (a soluble

protein), yielding a novel fusion protein, GST-CTBDH, that has been purified and shown to exhibit PC-selective phospholipid binding properties comparable to those of the complete BDH protein. Both GST-CTBDH and HH-Histag-BDH, a recently described purified recombinant form of human heart BDH (*14*), each bind to PC vesicles as demonstrated by sucrose gradient flotation studies (Figure 3) but fail to bind to DGDG vesicles. Both HH-Histag-BDH and GST-CTBDH also bind to PE/DPG vesicles, but such complexes are dissociated by treatment with salt, indicating a predominantly ionic (nonspecific) and relatively weak binding of these proteins to lipid vesicles that do not activate BDH. By contrast, the protein−PC complexes are not dissociated by treatment with salt, consistent with previous gel filtration studies of bovine heart BDH (*3*) and reflecting the specific interaction of BDH with PC as required for its activation. The two lipid binding proteins, HH-Histag-BDH and GST-CTBDH, exhibit a similar affinity for pyrenyl-PC (a lipid that activates BDH) as revealed by the quenching of tryptophan fluorescence afforded by titration with each of these fluorescent lipids in lipid bilayers (Figure 4 and Table 1). Both proteins have an affinity for pyrenyl-PE (a lipid that does not activate BDH) that is ∼15-fold lower than for pyrenyl-PC under similar conditions. Thus, GST-CTBDH and HH-Histag-BDH each exhibit similar PC-selective lipid binding properties that are characteristic of this PC-requiring enzyme.

The recombinant GST-CTBDH fusion protein (chimera) was expressed readily in *E. coli* but, of six detergents tested, only *N*-lauroylsarcosine efficiently solubilized the protein in a form that could be affinity purified (see Figure 2). By contrast with other GST fusion proteins (*30*), the addition of up to 4% Triton X-100 to the lysate (in *N*-lauroylsarcosine) did not enhance the yield of purified GST-CTBDH (30−40% recovery of the solubilized protein based on GST activity). After purification, GST-CTBDH is soluble (to ∼1 mg/mL) in the absence of detergent as are both bovine heart and rat liver BDH (*27*, *31*). GST-CTBDH is immunoreactive with both anti-BDH and anti-GST antibodies and migrates in SDS−PAGE at a size (37 kDa) approximating that calculated from its amino acid sequence (38 259 Da). By contrast, CTBDH (prepared by thrombin cleavage of GST-CTBDH) migrates faster in SDS−PAGE than expected (i.e., at about 7.5 kDa; see Figure 5) though its mass (12 111 Da by mass spectrometry) is identical to that predicted from its amino acid sequence. The anomalously fast migration of CTBDH on SDS−PAGE suggests a higher than average SDS binding that may be indicative of a hydrophobic or amphipathic character in this segment of BDH. While hydrophobic transmembrane helices are not evident in HH-BDH (*10*), amphipathic helical membrane anchors have been found or postulated in similar kinds of membrane proteins, e.g., prostaglandin H_2 synthase (*32*), 17β-hydroxysteroid dehydrogenase (*16*), and vinculin (*33*). Indeed, possible amphipathic helical elements within CTBDH (Duncan and McIntyre, unpublished) and/or predicted β-sheet structures (*10*) (both recognized motifs in proteins that bind to lipid bilayers; e.g., refs *34* and *35*) within this domain may contribute to the PC-specific lipid binding site of the enzyme. The apparently higher than average SDS binding to CTBDH is consistent with the herein demonstrated lipid binding properties of this domain of BDH.

Both HH-Histag-BDH and GST-CTBDH bind to lipid vesicles with characteristics that are similar to each other. The centrifugation studies show, for the first time, that BDH binds quantitatively to PC vesicles, forming a relatively homogeneous protein−PC complex that floats up through the sucrose gradient (see Figure 3). The fusion protein, GST-CTBDH, is similar in this regard to the complete protein, HH-Histag-BDH. By gel exclusion chromatography, both HH-Histag-BDH and GST-CTBDH were found to coelute with MPL vesicles (unpublished results). Thus, both BDH and GST-CTBDH bind to MPL (not shown) or PC vesicles (Figure 3). By contrast, neither HH-Histag-BDH nor GST-CTBDH binds to vesicles prepared from DGDG, an unsaturated lipid that forms bilayer vesicles with properties similar to those of dioleoyl-PC vesicles (*35*−*37*). The stability of complexes of either HH-Histag-BDH or GST-CTBDH reconstituted with PC/DPG vesicles to treatment with salt (up to 0.5 M LiBr or NaCl) and the salt dissociation of analogous complexes with PE/DPG vesicles are consistent with the lipid binding properties of purified bovine heart BDH (*3*). Both GST-CTBDH and HH-Histag-BDH exhibited a similar salt-dissociable interaction with PE/DPG vesicles, a mixture of phospholipids that does not serve to activate BDH. The salt-induced dissociation of such PE/DPG complexes appears referable to a physical change in the lipid, as indicated by increased turbidity or flocculation of such samples (also evident with PE/DPG vesicles in the absence of protein). By contrast, samples prepared with either PC or DGDG vesicles exhibited no apparent salt-induced changes in turbidity. The salt-stable binding of both HH-Histag-BDH and GST-CTBDH to PC vesicles, as demonstrated by the sucrose gradient flotation studies described here, reflects the lipid specificity of BDH with its requirement of PC for catalysis.

HH-Histag-BDH and GST-CTBDH have a similar affinity for PC as quantitated from the quenching of tryptophan fluorescence afforded by titration with pyrenyl-PC (Figure 4). Both proteins exhibit biphasic quenching profiles with most of the quenching being effected by a relatively low pyrenyl-PC concentration in the lipid vesicles (i.e., <2.5% of the total lipid). Although both the initial tryptophan fluorescence amplitudes (see Figure 4) and the number of tryptophans differ in HH-Histag-BDH and GST-CTBDH (five and seven, respectively, of which three are in CTBDH, at residues 215, 276, and 277), the amplitude of the fluorescence quenching, afforded by low pyrenyl-PC concentrations, is comparable for both proteins. Since tryptophan fluorescence quenching is not observed with GST, the quenching of GST-CTBDH presumably derives from energy transfer quenching arising from the interaction of pyrenyl-PC with one or more of the three tryptophans in the CTBDH domain of each protein (either in HH-Histag-BDH or in GST-CTBDH). For either protein, there is a fraction of the tryptophan fluorescence that is not quenched by even high concentrations of either pyrenyl-PC or pyrenyl-PE; this nonquenchable fluorescence is likely referable to the tryptophan located in the aqueous domains of the proteins.

Both HH-Histag-BDH and GST-CTBDH exhibit similar effective Stern−Volmer quenching constants in the low (<2.5%) pyrenyl-PC concentration range (see Table 1) such that half-maximal quenching is effected by ∼0.1% pyrenyl-PC. Given a lipid to protein molar ratio of ∼100, the

fluorescence quenching afforded by low pyrenyl-PC is in the range that approximates stoichiometric interaction between the pyrenyl-PC and protein. Therefore, this may reflect the direct binding of pyrenyl-PC to HH-Histag-BDH or to GST-CTBDH especially since only a small amount of quenching (~10%) is observed in control studies with 1% pyrenyl-PC in PC/DPG vesicles (not shown). In the higher pyrenyl-PC concentration range (>2.5%) in PE/DPG vesicles, there is additional tryptophan fluorescence quenching that results in a total fractional quenching comparable to that obtained by titration with pyrenyl-PE (a fluorescent lipid that does not activate BDH). The tryptophan fluorescence quenching afforded by titration with pyrenyl-PE (and presumably also by the higher concentration range of pyrenyl-PC) likely results from the nonspecific interaction of bilayer lipids with CTBDH present in either HH-Histag-BDH or GST-CTBDH. In similar previous studies of bovine heart BDH (*6*), quenching of tryptophan fluorescence by pyrenyl-PC was reported to be almost complete at about 25 mol % pyrenyl-PC and to exhibit a homogeneous quenching profile with half-maximal quenching at ~6 mol % of total lipid. However, in those prior studies, the low pyrenyl-PC concentration range (<1%) was not systematically explored, and the data exhibited significant scatter such that a biphasic process could not be excluded (*6*). In the studies described here, both HH-Histag-BDH and GST-CTBDH exhibit maximal tryptophan fluorescence quenching that is comparable with both pyrenyl-PC and pyrenyl-PE. Likewise, the Stern−Volmer quenching constants with each type of lipid, either pyrenyl-PC or pyrenyl-PE, are similar, such that each protein has an ~15-fold higher affinity for the PC versus PE analogue, a selectivity consistent with the requirement of PC for the activation of BDH. The quenching by pyrenyl-PE appears to reflect nonspecific interaction of phospholipid with BDH or CTBDH in the lipid bilayer. The more efficient quenching afforded by pyrenyl-PC is indicative of a high-affinity interaction with PC that reflects the specificity of BDH for this lipid. These results are consistent with the two-step lipid binding model for the activation of BDH by PC (*6*).

The finding that CTBDH confers PC-specific binding to GST validates the concept that these 103 amino acid residues constitute the lipid binding domain of BDH (*10*). A similar GST fusion protein strategy has been used to identify a novel conserved 55-residue motif in the tail domain of vinculin that mediates its insertion into acidic phospholipid bilayers and includes predicted amphipathic helices (*33*). Early studies showed that, although the specificity for activation of BDH is determined by the chemical structure of the polar head of the lipid, the binding of PC to BDH is driven by hydrophobic interaction with the fatty acyl chains (*3*, *4*, *8*). Fluorescence studies also had indicated both specific and nonspecific lipid binding sites on BDH (*42*). Deletion of several C-terminal residues from BDH, either by proteolysis (*17*, *43*) or by mutagenesis (*12*, *18*), was shown to markedly reduce catalysis. Carboxypeptidase cleavage of BDH prevented its activation by either bilayer or soluble PC (*17*), and a BDH deletion mutant (with a truncated and modified C-terminus) exhibited altered lipid binding kinetics and low activity consistent with loss of activation by PC (*18*). Taken together, these results suggest distinct sites for lipid binding and PC specificity and are consistent with the two-step mechanism for the activation of BDH by PC in bilayers (*6*). In contrast to studies of truncated forms of BDH that have been shown to manifest a loss of PC-dependent activation (*12*, *18*), the work reported here demonstrates that CTBDH confers the PC-specific lipid binding properties of BDH to an otherwise soluble protein, GST. The results show that CTBDH includes both the general lipid binding and PC-specific sites evident in BDH, with GST-CTBDH exhibiting GST catalytic activity and PC-specific lipid binding properties. The thrombin-specific cleavage site (in the link between the GST and CTBDH domains) is accessible to proteolysis (see Figure 5) with the rate of cleavage being the same in the presence and absence of PC vesicles, indicating that the interdomain link is not embedded in the lipid bilayer. In the absence of covalently bound GST, the CTBDH domain, prepared by thrombin cleavage of GST-CTBDH (either before or after reconstitution with PC vesicles), retains its lipid binding properties. The affinity of GST-CTBDH for PC, as revealed by pyrenyl-PC quenching of tryptophan fluorescence, is comparable to that of fully active recombinant HH-Histag-BDH. Therefore, this domain of BDH includes both the PC-specific site [that appears to be near the C-terminus (*12*, *17*, *18*)] and the binding site for the fatty acyl chains that drives the binding of PC to BDH (*3*, *4*, *8*). The studies reported here show, for the first time, that CTBDH, the 103-residue C-terminal segment of BDH, constitutes a PC-selective lipid binding domain of this PC-requiring enzyme.

ACKNOWLEDGMENT

We thank Charles Goldthwaite for assistance in purifying GST-CTBDH and HH-Histag-BDH and Kim Tran for technical assistance. We also thank Dr. Joe Beechem for advice on analysis of the fluorescence quenching data, Dr. Viet Q. Nguyen of the Vanderbilt University Mass Spectrometry Research Center for expert assistance in the acquisition and interpretation of MALDI mass spectra, and Dr. Richard Caprioli for advice on mass spectrometry. We acknowledge the Vanderbilt Cancer Center Sequencing Laboratory for sequencing the PCR fragment.

REFERENCES

1. McIntyre, J. O., Bock, H.-G., and Fleischer, S. (1978) *Biochim. Biophys. Acta 513*, 255−267.
2. Fleischer, B., Casu, A., and Fleischer, S. (1966) *Biochem. Biophys. Res. Commun. 24*, 189−193.
3. Gazzotti, P., Bock, H. G., and Fleischer, S. (1975) *J. Biol. Chem. 250*, 5782−5790.
4. Grover, A. K., Slotboom, A. J., De Haas, G. H., and Hammes, G. G. (1975) *J. Biol. Chem. 250*, 31−38.
5. Fleischer, S., and McIntyre, J. O. (1985) in *Achievements and Perspectives in Mitochondrial Research* (Quagliariello, E., and Palmieri, F., Eds.) pp 347−356, Elsevier Science Publishers BV, Amsterdam.
6. Sandermann, H., McIntyre, J. O., and Fleischer, S. (1986) *J. Biol. Chem. 261*, 6201−6208.
7. Rudy, B., Dubois, H., Mink, R., Trommer, W. E., McIntyre, J. O., and Fleischer, S. (1989) *Biochemistry 28*, 5354−5366.
8. Cortese, J. D., Vidal, J. C., Churchill, P., McIntyre, J. O., and Fleischer, S. (1982) *Biochemistry 16*, 3899−3908.
9. Isaacson, Y. A., Deroo, P. W., Rosenthal, A. F., Bittman, R., McIntyre, J. O., Bock, H.-G., Gazzotti, P., and Fleischer, S. (1979) *J. Biol. Chem. 254*, 117−126.
10. Marks, A. R., McIntyre, J. O., Duncan, T. M., Erdjument-Bromage, H., Tempst, P., and Fleischer, S. (1992) *J. Biol. Chem. 267*, 15459−15463.

11. Churchill, P., Hempel, J., Romovacek, H., Zhang, W.-W., Brennan., and Churchill, S. (1992) *Biochemistry 31*, 3793−3799.
12. Green, D., Marks, A. R., Fleischer, S., and McIntyre, J. O. (1996) *Biochemistry 35*, 8158−8165.
13. Persson, B., Krook, M., and Jornvall, H. (1991) *Eur. J. Biochem. 200*, 537−543.
14. Chelius, D., Loeb-Hennard, C., Fleischer, S., McIntyre, J. O., Marks, A. R., Moeller, J., Hahn, S., Philipp, R., Wise, J. G., and Trommer, W. E. (2000) *Biochemistry 39*, 9687−9697.
15. Ghosh, D., Weeks, C. M., Grochulski, P., Duax, W. L., Erman, M., Rimsay, R. L., and Orr, J. C. (1991) *Proc. Natl. Acad. Sci. U.S.A. 88*, 10064−10068.
16. Ghosh, D., Pletnev, V. Z., Zhu, D. W., Wawrzak, Z., Duax, W. L., Pangborn, W., Labrie, F., and Lin, S. X. (1995) *Structure 3*, 503−513.
17. Adami, P., Duncan, T. M., McIntyre, J. O., Carter, C. E., Fu, C., Melin, M., Latruffe, N., and Fleischer, S. (1993) *Biochem. J. 292*, 863−872.
18. Langston, H. P., Jones, L., Churchill, S., and Churchill, P. F. (1996) *Arch. Biochem. Biophys. 327*, 45−52.
19. Lowry, O. H., Rosebrough, N. J., Farr, A. L., and Randall, R. J. (1951) *J. Biol. Chem. 193*, 265−275.
20. Sambrook, J., Fritsch, E. F., and Maniatis, T. (1989) *Molecular Cloning: A Laboratory Manual*, 2nd ed., Cold Spring Harbor Laboratory, Cold Spring Harbor, NY.
21. Seifter, S., Dayton, S., Novic, B., and Muntwyler, E. (1950) *Arch. Biochem. Biophys. 25*, 191−200.
22. Laemmli, U. K. (1970) *Nature 227*, 680−685.
23. Cortese, J. D., McIntyre, J. O., Duncan, T. M., and Fleischer, S. (1989) *Biochemistry 28*, 3000−3008.
24. Eibl, H.-J., McIntyre, J. O., Fleer, E. A. M., and Fleischer, S. (1983) *Methods Enzymol. 98*, 623−632.
25. Lakowicz, J. R. (1983) *Principles of Fluorescence Spectroscopy*, Plenum Press, New York.
26. Lehrer, S. S. (1971) *Biochemistry 10*, 3254−3263.
27. McIntyre, J. O., Latruffe, N., Brenner, S. C., and Fleischer, S. (1988) *Arch. Biochem. Biophys. 262*, 85−98.
28. Zhang, H., Stoeckli, M., Andren, P. E., Caprioli, R. M. (1999) *J. Mass Spectrom. 34*, 377−383.
29. Wu, L., Einstein, M., Geissler, W. M., Chan, H. K., Elliston, K. O., and Andersson, S. (1993) *J. Biol. Chem. 268*, 12964−12969.
30. Frangioni, J. V., and Neel, B. G. (1993) *Anal. Biochem. 210*, 179−187.
31. Bock, H.-G., and Fleischer, S. (1975) *J. Biol. Chem. 250*, 5774−5781.
32. Picot, D., Loll, J. P., and Garavito, R. M. (1994) *Nature 367*, 243−249.
33. Johnson, R. P., Niggli, V., Durrer, P., and Craig, S. W. (1998) *Biochemistry 37*, 10211−10222.
34. Tamm, L. K. (1994) in *Peptide−Bilayer Interactions in Membrane Protein Structure* (White, S. H., Ed.) pp 283−313, Oxford University Press, New York and Oxford.
35. Sue, S.-C., Rajan, P. K., Chen, T.-S., Hsieh, C.-H., and Wu, W.-G. (1997) *Biochemistry 36*, 9826−9836.
36. Gennis, R. B. (1989) in *Biomembranes: molecular structure and function* (Cantor, R. C., Ed.) Springer-Verlag, New York.
37. Marsh, D. (1990) *Handbook of Lipid Bilayers*, CRC Press, Boca Raton, FL.
38. Koynova, R., and Caffrey, M. (1994) *Chem. Phys. Lipids 69*, 181−207.
39. McIntyre, J. O., Churchill, P., Maurer, A., Berenski, C. J., Jung, C. Y., and Fleischer, S. (1983) *J. Biol. Chem. 258*, 953−959.
40. Newton, A. C., and Johnson, J. E. (1998) *Biochim. Biophys. Acta 1376*, 155−172.
41. Klein, K., Rudy, B., McIntyre, J. O., Fleischer, S., and Trommer, W. E. (1996) *Biochemistry 35*, 3044−3049.
42. Wang, S., Martin, E., Cimino, J., Omann, G., and Glaser, M. (1988) *Biochemistry 27*, 2033−2039.
43. Maurer, A., McIntyre, J. O., Churchill, S., and Fleischer, S. (1985) *J. Biol. Chem. 260*, 1661−1669.

BI000425Y